INTERNATIONAL JOURNAL FOR NUMERICAL METHODS IN FLUIDS, VOL. 8, 1367–1388 (1988)

A UNIFIED APPROACH TO DIRECT AND INVERSE BOUNDARY LAYER SOLUTIONS

K. C. KAUFMAN* AND G. H. HOFFMAN

Applied Research Laboratory, The Pennsylvania State University, Post Office Box 30, State College, PA 16804, U.S.A.

SUMMARY

A unified approach is presented for solving the two-dimensional incompressible boundary layer equations. Solutions are obtained for direct and inverse options using the same equation formulation by a simple interchange of boundary conditions. A modified form of the mechul function scheme obtains inverse solutions with specification of transformed wall shear, skin friction coefficient or displacement thickness distributions. Direct solutions may be obtained without altering the block tridiagonal structure of the system by simply requiring no corrections on the streamwise pressure gradient parameter. Fourth-order spline discretization approximates normal derivatives with two- and three-point backward differences approximating streamwise derivatives, yielding a fully implicit solution method. The resulting spline/finite difference equations are solved by Newton–Raphson iteration together with partial pivoting. The results of the study demonstrate the importance of proper linearization of all equations. The successful use of spline discretization is also tied to the use of strong two-point boundary conditions at the wall for cases involving reversed flow. Numerical solutions are presented for several non-similar flows and compared with published results.

KEY WORDS Laminar boundary layer Splines Incompressible Inverse and direct methods

INTRODUCTION

The calculation of boundary layer flows is usually divided into two distinct categories, direct and inverse methods. The direct method, which involves specifying a pressure or inviscid velocity distribution over the body, has been widely used for many years. The pioneering work of Smith and Clutter[1] is an excellent example of a direct boundary layer solution. This approach performs well for attached shear layers, but cannot treat separating boundary layers because of the singularity that exists at the separation point when the edge velocity is specified.[2,3] This singularity prevents the use of the direct method for regions of backflow, including separation bubbles and trailing edge separation.

To obtain solutions for separated boundary layers, several types of inverse methods have been developed. By specifying distributions of displacement thickness, wall shear or similar quantities, and obtaining the streamwise pressure distribution, these methods eliminate the singularity in the boundary layer equations at separation. The equations of motion may then be integrated through the region of separation under the condition that the extent of separation is small (backflow velocities less than 10% of the edge velocity). The boundary layer equations remain valid under the assumption that the shear layer is thin ($d\delta/dx \ll 1$). For shear layers which violate this

* Present address: General Dynamics, Electric Boat Division, Groton, CN 06340, U.S.A.

0271–2091/88/111367–22$11.00
© 1988 by John Wiley & Sons, Ltd.
Received 24 June 1987
Revised 15 January 1988

condition, upstream influences become significant and the boundary layer equations alone can no longer accurately describe the flow.

Catherall and Mangler[4] originated the inverse procedure, specifying a displacement thickness distribution near the separation point to obtain regular solutions into a region of backflow. Once inside the separated zone, however, the procedure developed instabilities which required a progressive increase in convergence limits as the solution continued downstream. Since the boundary layer equations are parabolic, these instabilities arise from marching in a direction opposite to the streamwise velocity.

Reyhner and Flugge-Lotz[5] developed the FLARE approximation which eliminates these instabilities by setting all streamwise convection terms to zero inside the region of backflow. The x-convective terms are small in this region for thin separated zones, so this introduces only minor errors while allowing a forward-marching procedure to continue through the separated region. Since it was presented, the FLARE approximation has been a standard part of the majority of inverse methods which seek to resolve regions of separated flow.

An iterative procedure developed by Williams[6] improved on the FLARE approach by making repeated downstream and upstream passes through the separated zone. On the first pass, FLARE is used to define the extent of the separation zone. An upstream pass, using a direct solution, is made inside the region of backflow to determine the convective terms. The downstream pass is then repeated without FLARE, using the results obtained from the upstream solution. This process is repeated for several cycles until convergence is reached. The DUIT (downstream–upstream iteration) procedure produces more accurate velocity profiles for the separated region and has been used successfully by Cebeci *et al.*[7] A drawback inherent in the iterative process is that only closed separation bubbles or separated regions which reach an asymptotic state can be treated.

A variety of inverse studies have appeared in the literature.[8-16] The quantities specified by these methods vary, with the majority specifying the Reynolds scaled displacement thickness or the wall shear. Most are able to specify only one quantity. The work of Cebeci[15] is one significant exception. Cebeci considers the specification of skin friction coefficient and displacement thickness with a minimum of reformulation. An additional noteworthy paper is the study by Edwards and Carter,[16] where a unified approach to boundary layer solutions is presented in connection with interacting boundary layer theory. In Reference 16, displacement thickness is used to link the quasi-simultaneous viscous–inviscid interaction procedure.

This study presents a unified approach to the numerical solution of the direct and inverse formulations of the laminar boundary layer equations using an implicit spline/finite difference discretization scheme. The method is formulated to allow the specification of transformed wall shear, skin friction coefficients or displacement thickness distributions for inverse solutions by simply switching the appropriate boundary conditions. This idea is similar to the work of Cebeci.[15] The current study goes beyond that of Cebeci by also allowing direct or inverse solutions to be obtained with the same technique. Thus the present work is truly unified in handling direct as well as shear or displacement thickness inverse solutions with the same formulation, requiring only minor changes in the boundary conditions depending upon the desired solution.

The present scheme applies fourth-order splines, as derived by Rubin and Khosla,[17] to approximate the normal derivatives in the boundary layer equations, with two- and three-point backward differences to discretize the streamwise derivatives. The differencing scheme was chosen to yield a fully implicit solution method. The splines also provide increased accuracy for a given number of mesh points. (All spline notation is in the form given in Reference 17.)

The mechul function method, originally devised for inverse methods by Cebeci and Keller,[18] is

used in a modified form described by Kaufman and Hoffman.[19] This modified form is necessary because of the use of the spline discretization. The FLARE approximation is employed in separation zones to prevent development of instabilities inherent in marching downstream through regions of reversed flow.

Following discretization, the non-linear spline/finite difference equations are linearized and solved using Newton's method. The resulting linear block tridiagonal matrix system for the solution vector corrections at each streamwise station is solved using L–U decomposition. Partial pivoting is necessary in the block tridiagonal solution process to prevent the build-up of round-off errors.

GOVERNING EQUATIONS

The governing equations for a steady, incompressible, two-dimensional laminar boundary layer in dimensionless, Reynolds number scaled form are

$$\text{continuity} \qquad \frac{\partial u}{\partial x}+\frac{\partial V}{\partial Y}=0, \tag{1}$$

$$x\text{-momentum} \qquad u\frac{\partial u}{\partial x}+V\frac{\partial u}{\partial Y}=-\frac{\partial p}{\partial x}+\frac{\partial u^2}{\partial Y^2}, \tag{2}$$

$$y\text{-momentum} \qquad \frac{\partial p}{\partial Y}=0, \tag{3}$$

and the Euler equation applied at the body surface gives

$$-\frac{\mathrm{d}p_e}{\mathrm{d}x}=u_e\frac{\mathrm{d}u_e}{\mathrm{d}x}.$$

The usual boundary conditions are

$$\text{impervious wall} \qquad \psi(x,0)=0, \tag{4a}$$

$$\text{no-slip} \qquad u(x,0)=0, \tag{4b}$$

$$\text{far field} \qquad u(x,Y)\to 1 \quad \text{as} \quad Y\to\infty, \tag{4c}$$

where the stream function is defined by

$$u=\frac{\partial\psi}{\partial Y}, \qquad V=-\frac{\partial\psi}{\partial x}. \tag{5}$$

The introduction of the stream function identically satisfies continuity, equation (1).

For a direct solution of the boundary layer equations, an edge velocity or pressure coefficient distribution is typically specified. Inverse solutions of the boundary layer equations can be obtained by specifying either a wall shear (or function of the wall shear) or a displacement thickness distribution. The form of the resulting boundary conditions will be discussed later.

To capture boundary layer growth, the governing equation (1)–(3) and the boundary conditions (4) and (5) are transformed using the Levy–Lees pseudo-self-similar transformation given by

$$\xi(x)=\int_0^x u_e\,\mathrm{d}x, \tag{6a}$$

$$\eta(x,Y)=\frac{u_e}{\sqrt{(2\xi)}}Y. \tag{6b}$$

A psuedo-self-similar stream function is defined as

$$\psi(x, Y)=\sqrt{(2\xi)}f(\xi, \eta). \tag{7}$$

The introduction of equation (7) also removes the leading edge singularity and allows a self-starting solution.

Transforming the velocity components and the x- and y-derivatives, equation (2) becomes

$$f_{\eta\eta\eta}+ff_{\eta\eta}+\beta(1-f_\eta^2)=2\xi\,[f_\eta f_{\eta\xi}-f_\xi f_{\eta\eta}], \tag{8}$$

where β is the streamwise pressure gradient parameter defined as

$$\beta(\xi)=\frac{2\xi}{u_e}\frac{\mathrm{d}u_e}{\mathrm{d}\xi}. \tag{9}$$

By setting $\xi=0$, equation (8) reduces to the Falkner–Skan equation, with no dependence on ξ. The ODE may be solved for any Falkner–Skan solution, or a starting solution may be obtained for a non-similar flow.

The FLARE approximation is usually applied to the untransformed x-momentum equation (2) defining a FLARE coefficient θ:

$$\theta u\frac{\partial u}{\partial x}+V\frac{\partial u}{\partial Y}=u_e\frac{\mathrm{d}u_e}{\mathrm{d}x}+\frac{\partial^2 u}{\partial Y^2},$$

where

$$\theta=\begin{cases}1, & u\geqslant 0,\\ 0, & u\leqslant 0.\end{cases}$$

Horton,[11] however, notes that when using psuedo-self-similar variables this approach is too restrictive, since it affects the self-similar as well as the non-similar solutions. Since the streamwise convection term introduces the instabilities in regions of reversed flow, only the analogous transformed term needs to be removed. The FLARE coefficient is applied only to the $f_\eta f_{\eta\xi}$ term, and equation (8) becomes

$$f_{\eta\eta\eta}+ff_{\eta}+\beta(1-f_\eta^2)=2\xi\,[\theta f_\eta f_{\eta\xi}-f_\xi f_{\eta\eta}], \tag{10}$$

where

$$\theta=\begin{cases}1, & f_\eta\geqslant 0,\\ 0, & f_\eta\leqslant 0.\end{cases}$$

Here, when ξ is set to zero for a Falkner–Skan solution, no θ-terms remain which would interfere with obtaining the self-similar solution that is sought. Horton's form is used in the present work.

The transformed boundary conditions are

$$f(\xi, 0)=f_\eta(\xi, 0)=0, \tag{11a}$$

$$f_\eta(\xi, \eta)=1 \quad \text{as} \quad \eta\to\eta_\infty. \tag{11b}$$

For an inverse solution, an additional boundary condition is added which consists of specifying wall shear, displacement thickness or another quantity. Since the streamwise pressure gradient parameter is unknown, the system is overdetermined. To close the system, Cebeci and Keller[18] introduce an additional differential equation by letting

$$\beta(\xi)=\beta(\xi, \eta)$$

and then requiring

$$\partial\beta/\partial\eta=0. \tag{12}$$

Equation (12) provides the additional relation needed to close the system of equations for an inverse solution.

While this formulation of the mechul function method was applied in Reference 18, Kaufman and Hoffman[19] discovered that, when applying a spline/finite difference scheme (particularly spline $S^1(4,0)$[17]) to the mechul function method, equation (12) resulted in a singular matrix. This singularity was due totally to the form of the spline relations. To prevent this problem, the auxiliary equation is changed to

$$\partial^2\beta/\partial\eta^2=0, \tag{13}$$

with equation (12) enforced through the boundary conditions.

In order to apply spline $S^1(4,0)$ repeatedly, the momentum equation is written as three first-order equations. The complete set, including the auxiliary mechul function equation, is

$$f_\eta=u, \tag{14a}$$
$$u_\eta=G, \tag{14b}$$
$$G_\eta+fG+\beta(1-u^2)=2\xi[\theta uu_\xi-Gf_\xi], \tag{14c}$$
$$\beta_{\eta\eta}=0, \tag{14d}$$

with the boundary conditions

$$f(\xi,0)=u(\xi,0)=0, \tag{15a}$$
$$u(\xi,\eta)\to 1 \quad \text{as} \quad \eta\to\eta_\infty, \tag{15b}$$

while equation (12) is enforced at the wall or the far field as needed.

The system of inverse boundary layer equations can also be used for a direct boundary layer solution. For the standard direct boundary layer problem, the streamwise pressure gradient is given, either explicitly or by specifying u_e or C_p, and β is treated as a fixed parameter at each streamwise station.

For the system of equations considered here, β is a variable to be obtained during the solution process. Thus, to solve a direct case using this system, an additional boundary condition must be specified which sets β at each streamwise station. The appropriate boundary conditions are then

$$f(\xi,0)=u(\xi,0)=0, \tag{16a}$$
$$u(\xi,\eta_\infty)=1, \tag{16b}$$
$$\beta(\xi,\eta_\infty)=\beta(\xi). \tag{16c}$$

Here, equation (16c) takes the place of the inverse boundary condition discussed previously.

For the additional boundary condition required by an inverse solution, three possibilities are treated in this paper (two for skin friction and one for displacement thickness).

For the inverse solutions of Keller and Cebeci,[8,18] where the mechul function is introduced, Horton[10] and Kaufman and Hoffman[19] specify the self-similar form of the wall shear, given by f''_w (where primes denote differentiation with respect to η). This is by far the simplest of the inverse boundary conditions when the equations are cast in similarity form. The boundary condition takes the form

$$f''_w=G_w=S(\xi). \tag{17}$$

Although equation (17) is the simplest condition to apply, it is not the most useful. From a physical standpoint, specification of a skin friction coefficient is more plausible. Here, a skin friction coefficient with one of two possible definitions is specified:

(1) skin friction coefficient based on the reference velocity,

$$C_{f_\infty} = \frac{\tau_w^*}{\frac{1}{2}\rho^*(u_\infty^*)^2};$$

(2) skin friction coefficient based on the boundary layer edge velocity,

$$C_{f_e} = \frac{\tau_w^*}{\frac{1}{2}\rho^*(u_e^*)^2}.$$

Transforming these definitions to similarity variables yields

$$C_{f_\infty}\sqrt{(Re)} = \frac{2u_e^2}{\sqrt{(2\xi)}} f_w'', \tag{18a}$$

$$C_{f_e}\sqrt{(Re)} = \frac{2}{\sqrt{(2\xi)}} f_w''. \tag{18b}$$

When either skin friction coefficient is specified, f_w'' no longer remains constant. Using equation (18), the boundary condition on f_w'' is thus obtained as a function of C_{f_e} or C_{f_∞}, u_e and ξ:

$$f_w'' = G_w = F(C_f, u_e, \xi). \tag{19}$$

The boundary condition then takes the form

$$G_w - F = 0. \tag{20}$$

The displacement thickness may also be specified, using a boundary condition at the far field instead of the wall condition used for the two previous inverse conditions. The standard definition of the displacement thickness is

$$\delta^* = \int_0^\infty \left(1 - \frac{u}{u_e}\right) dy. \tag{21}$$

Scaled and transformed to similarity variables, equation (21) becomes

$$\delta^*\sqrt{(Re)} = \frac{2\xi}{u_e}\int_0^{\eta_\infty} (1 - f')\, d\eta. \tag{22}$$

From this result, a transformed displacement thickness can be defined as

$$\hat{\delta}^* = \int_0^{\eta_\infty} (1 - f')\, d\eta. \tag{23}$$

Integrating across the boundary layer, the transformed displacement thickness provides the required inverse condition at the far field:

$$f \to \eta - \hat{\delta}^* \quad \text{as} \quad \eta \to \eta_\infty. \tag{24}$$

DISCRETIZED EQUATIONS

Since the discretization used here is almost identical to that in Reference 19, only the highlights in the present case will be given. The ξ-derivative in equation (14c) is first discretized using the

generalized backward difference formula

$$(\partial g/\partial \xi)_i = a g_i + b g_{i-1} + c g_{i-2},$$

and then the η-derivatives in equation (14) are replaced by spline approximations. At nodal point (i, j) the result is

$$l^f_{ij} = u_{ij}, \tag{25a}$$

$$l^u_{ij} = G_{ij}, \tag{25b}$$

$$l^G_{ij} = \theta_{ij} C_{1_{ij}} u^2_{ij} + C_{2_{ij}} f_{ij} G_{ij} + \beta_{ij}(u^2_{ij} - 1) + C_{3_{ij}} G_{ij} + \theta_{ij} C_{4_{ij}}, \tag{25c}$$

$$L^\beta_{ij} = 0, \tag{25d}$$

where C_1, C_2, C_3 and C_4 are functions of ξ_i, a, b, c, and f_{i-1}, f_{i-2}, u_{i-1} and u_{i-2}.

In equation (25) there are eight unknowns, and hence four tridiagonal spline relations are required to close the system. $S^1(4, 0)$ is used to relate l^f to f, l^u to u and l^G to G; then $S^2(4, 0)$ is used to relate L^β to β. The expressions for $S^1(4, 0)$ and $S^2(4, 0)$ are given by equations (15) and (16) of Reference 19. The number of unknowns is then reduced to four by the use of equations (25a)–(25d) to eliminate l^f, l^u, l^G and L^β. The result is a block tridiagonal system for the unknowns f, u, G and β. Because of the non-linearity of the momentum equation, the entire system of equations must be linearized for solution by the Newton–Raphson technique.

The block tridiagonal correction equations may be written in the following matrix form (i subscript understood):

$$\mathbf{B}_j \mathbf{Z}_{j-1} + \mathbf{A}_j \mathbf{Z}_j + \mathbf{C}_j Z_{j+1} = \mathbf{R}_j \tag{26}$$

for $2 \leqslant j \leqslant N$, where N is the number of intervals in η and

$$\mathbf{Z}_j = [\delta f, \delta u, \delta G, \delta \beta]^T_j. \tag{27}$$

As in Reference 19, $\mathbf{A}_j$, $\mathbf{B}_j$ and $\mathbf{C}_j$ are 4×4 matrices whose elements are obtained from the four correction equations, and $\mathbf{R}_j$ is a four-component column vector of known quantities from the right-hand sides of the correction equations.

To close the block tridiagonal system, four boundary conditions must be supplied at both the wall and far field. When an insufficient number of physical conditions exists, numerical conditions obtained from two-point spline relations are added to the system. The numerical implementation of the boundary conditions for the inverse shear and displacement thickness methods and the direct method will now be covered in detail.

Using index notation (with i understood), the boundary conditions common to both the direct and inverse formulations are

$$f_1 = 0, \tag{28a}$$

$$u_1 = 0, \tag{28b}$$

$$u_{N+1} = 1. \tag{28c}$$

The remaining boundary condition depends on the formulation.

Wall shear boundary conditions

The three possible boundary conditions in the wall shear case are as follows:

$$G_1 - S = 0, \qquad f''_w \text{ specified}, \tag{29a}$$

or

$$G_1 - \tfrac{1}{2}\sqrt{(2\xi)}C_{f_e}\sqrt{(Re)} = 0, \qquad C_{f_e}\sqrt{(Re)} \quad \text{specified,} \tag{29b}$$

or

$$G_1 - \frac{1}{2}\frac{\sqrt{(2\xi)}}{u_e^2}C_{f_\infty}\sqrt{(Re)} = 0, \qquad C_{f_\infty}\sqrt{(Re)} \quad \text{specified.} \tag{29c}$$

The system at the wall is complete for any of the shear cases by the specification of the derivative condition on β:

$$\beta_\eta(\xi, \eta) = 0.$$

This equation, when approximated by a two-point spline relation, reduces to

$$\beta_2 - \beta_1 = 0. \tag{30}$$

Since only one boundary condition exists in the far field, the two-point relation, equation (16) of Rubin and Khosla,[17] must be used three times, once each for f, u and G. Since G and its normal derivatives approach zero exponentially rapidly near the boundary layer edge, the difference $G''_{N+1} - G''_N$ is expected to be small and hence is neglected, leaving for the G condition

$$G_{N+1} - G_N - \frac{h_{N+1}}{2}(G'_{N+1} + G'_N) = 0. \tag{31}$$

The first and second derivatives in these equations can be eliminated by substitution from the appropriate equations.

Displacement thickness boundary conditions

When the displacement thickness method is used, the boundary conditions described in the previous subsection must be altered, both at the wall and far field. The inverse condition for the displacement thickness method is implemented at the boundary layer edge. Thus equation (20) must be replaced by a two-point spline relation and one spline condition at the far field must be discarded to allow for the condition on δ^*.

The two-point spline relation chosen for the wall is

$$f_2 - f_1 - \frac{h_2}{2}(u_2 + u_1) + \frac{h_2^2}{12}(G_2 - G_1) = 0. \tag{32}$$

This condition is identical to one of the conditions applied at the far field for the shear case. In the far field, the spline condition of f is replaced by

$$f_{N+1} - \eta_{N+1} + \delta^* = 0 \tag{33a}$$

or

$$f_{N+1} - \eta_{N+1} + \frac{u_e}{\sqrt{(2\xi)}}\delta^*\sqrt{(Re)} = 0, \tag{33b}$$

depending upon whether the transformed or untransformed displacement thickness is specified.

Direct boundary conditions

For the direct case, a slightly different set of boundary conditions is used. At the wall, the conditions are identical to those used for the displacement thickness method. At the boundary

layer edge, two physical conditions are given: equation (15b), which is always specified regardless of method, and equation (16c). Two-point spline relations are required to close the system.

It is apparent, considering the previous discussion, that only minor modifications need to be made to the boundary conditions even though a range of methods is treated. This is quite surprising and also quite helpful, since it allows the various methods to be combined into a single computer code with little difficulty.

It should also be noted that while only minor changes to the boundary conditions are required, very few other possibilities exist when using the two-point spline relations. The conditions obtained in the above sections consist of all available conditions for the current problem without further differentiating the momentum equation (which would greatly increase the complexity of the boundary conditions).

Linearized numerical boundary conditions

For the transformed wall shear case, the correction form of equation (29a) is simply

$$\delta G_1 = 0,$$

since $S(\xi)$ is given constant at each streamwise station. When C_{f_e} or C_{f_∞} is specified, the function $\bar{F}$ in equation (19) varies as the solution converges, since it is dependent upon ξ and, for the C_{f_∞} case, u_e. Thus F must be linearized. Equation (20) can be written in linearized form as

$$\delta G_1 - (F_{C_f}\delta C_f + F_{u_e}\delta u_e + F_\xi \delta\xi) = 0, \tag{34}$$

where δC_f is zero since C_f is specified. The partial derivatives of F, F_ξ and F_{u_e}, for specified C_{f_∞} are easily found from the definition of F.

The correction $\delta\xi$ is obtained from the definition of ξ, equation (6a):

$$\delta\xi_i = \frac{\Delta x}{2}\delta u_{e_i}. \tag{35a}$$

The correction δu_e is obtained from equation (41), the relation used to update u_e after each iteration (discussed later in this paper). The result is

$$\delta u_{e_i} = \frac{1}{4}\left[\left(\frac{\beta_{i-1}+\beta_i}{\xi_i}\right)\delta\xi_i + \left(\ln\frac{\xi_i}{\xi_{i-1}}\right)\delta\beta_i\right]. \tag{35b}$$

Equations (35) are solved for $\delta\xi_i$ and δu_{e_i} in terms of $\delta\beta_i$, yielding

$$\delta\xi_i = \frac{t_1 t_3}{1 - t_1 t_2}\delta\beta_i, \tag{36a}$$

$$\delta u_{e_i} = \frac{u_{e_i} t_3}{4(1 - t_1 t_2)}\delta\beta_i, \tag{36b}$$

where

$$t_1 = \frac{\Delta x}{8}u_{e_i},$$

$$t_2 = \frac{1}{\xi_i}(\beta_{i-1} + \beta_i),$$

$$t_3 = \ln(\xi_i/\xi_{i-1}).$$

Upon substitution of equations (36) into equation (34), the correction boundary condition takes the form

$$\delta G_1 - \lambda \delta \beta_1 = 0, \tag{37a}$$

where

$$\lambda = F_{u_e}\left(\frac{u_{e_i} t_3}{4(1-t_1 t_2)}\right) + F_\xi\left(\frac{t_1 t_3}{1-t_1 t_2}\right). \tag{37b}$$

For the displacement thickness method, a similar procedure is followed, except that the resulting boundary condition contains δf instead of δG. The final form is given by

$$\delta f_{N+1} + \lambda \delta \beta_{N+1} = \eta_{N+1} - f_{N+1} - \frac{u_e}{\sqrt{(2\xi)}} \delta^* \sqrt{(Re)}, \tag{38}$$

where λ is given by equation (37b) and F_ξ and F_{u_e} are the appropriate partial derivatives for the displacement thickness boundary condition.

Linearization of the associated two-point spline relations is straightforward. The resulting system of corrections at the boundaries can be written in block matrix form for the cases considered here as follows:

$$\mathbf{A}_1 \mathbf{Z}_1 + \mathbf{C}_1 Z_2 = \mathbf{R}_1 \tag{39}$$

$$\mathbf{B}_{N+1} \mathbf{Z}_N + \mathbf{A}_{N+1} \mathbf{Z}_{N+1} = \mathbf{R}_{N+1}. \tag{40}$$

The coefficients in equations (39) and (40) are 4×4 matrices and $\mathbf{Z}$ and $\mathbf{R}$ are four-component column vectors, as defined previously.

Solution procedure

The solution of the block tridiagonal system, equations (26), (39) and (40), is accomplished using L–U decomposition with partial pivoting in the blocks, exactly the same procedure as used in Reference 19. A more complete discussion of the matrix solution method is given in References 20 and 22.

The convergence criterion, applied to the corrections at each nodal point for station i, is

$$|g_j^{(n+1)} - g_j^{(n)}| = |\delta g_j^{(n)}| \leqslant 10^{-8}, \quad i \leqslant j \leqslant N+1,$$

for g equal to f, u, G and β. The block tridiagonal solution process is repeated at a streamwise station i, updating the solution variables with each iteration until the above criterion is met.

The transformed psuedo-self-similar form of the equations allows the solution procedure to be self-starting. Typically, the solution is started from either a flat plate or stagnation point flow, at which point the governing system reduces to ordinary differential equations.

As an initial guess to the starting solution, a fourth-order Pohlhausen polynomial is used to approximate the self-similar profiles of the solution variables. With the initial conditions provided by the Pohlhausen polynomial, the starting solution is obtained by solving the ODE system with the standard block method. This procedure can also be used to obtain any Falkner–Skan self-similar solution. If a non-similar solution is to be obtained, two-point backward differences, to approximate the ξ-derivatives, are used for the second station. Past the second streamwise station, three-point backward differences are ordinarily used.

Calculation of the edge velocity

An accurate method of determining the edge velocity is important, since u_e is an important characteristic of the boundary layer flow and would be required if the present method were

extended to a turbulent boundary layer or a viscous–inviscid iteration procedure. The edge velocity cannot, however, be determined directly from the solution procedure. For this formulation, u_e must be obtained through an integration of the solution variables.

The pressure gradient parameter is defined by equation (9). Noting that this is a double logarithmic derivative, equation (9) can be recast as

$$\tfrac{1}{2}\beta = \mathrm{d}(\ln u_e)/\mathrm{d}(\ln \xi). \tag{41}$$

Rearranging and integrating this result over the numerical interval $i-1$ to i yields

$$\ln(u_{e_i}/u_{e_{i+1}}) = \frac{1}{2}\int_{i-1}^{i} \beta \, \mathrm{d}(\ln \xi).$$

The right-hand side of this result may be approximated using the trapezoidal integration rule. The edge velocity at station i is then obtained from

$$u_{e_i} = u_{e_{i-1}} \mathrm{e}^{\Gamma}, \tag{42a}$$

where

$$\Gamma = \tfrac{1}{4}(\beta_i^{(n)} + \beta_{i-1}) \ln(\xi_i/\xi_{i-1}). \tag{42b}$$

The determination of u_e is problematical for a non-similar flow beginning with a stagnation point. To calculate subsequent edge velocity values, the value of u_e at $i=2$ must be input directly or estimated. This curious behaviour at the second streamwise station is due to the double logarithmic form of the pressure gradient definition.

The reason for this behaviour is apparent if the flow near the stagnation point is assumed to behave like a wedge flow.[23] Then the edge velocity is an exponential function of x such that (for $\beta = 1$)

$$u_e = cx^{\beta/(2-\beta)} = cx.$$

The constant c cannot be determined without specifying the body shape because of the pseudo-self-similar character of the flow. A similar observation was made by Bradshaw *et al.*,[24] who noted that it is necessary to provide the slope c near the stagnation point.

RESULTS

Numerical results for three laminar cases are presented using the present unified approach. These cases provide a test for all the direct and inverse formulations presented here. All calculations were made using a constant streamwise step size and a normal co-ordinate distribution determined by a geometric progression.

Howarth flow

A boundary layer with linearly decreasing edge velocity, the Howarth flow,[1,25] has become a well known test case for boundary layer computations and is included here mainly as a test for the direct method since no separation data are available. A tabular comparison of dimensionless wall shear values obtained by the present method and results from References 1, 26 and 27 are presented in Table I. The agreement is quite good, with the present method predicting separation at the same location as the above references.

Table I. Accuracy of direct method for Howarth flows

	Dimensionless wall shear $(\tau_w/\rho U_\infty^2)\sqrt{(Re)}$			
x	Present method	Howarth[26]	Smith–Clutter[1]	Cebeci–Smith[27]
0·1	0·968754	0·968382	—	0·968524
0·2	0·626548	0·626496	0·626249	0·626392
0·3	0·462782	0·462801	—	0·462645
0·4	0·357322	0·375442	0·357301	0·357197
0·5	0·279267	0·279307	—	0·279150
0·6	0·216228	0·216728	—	0·216119
0·7	0·161698	0·162281	—	0·161602
0·8	0·110977	0·111369	0·111516	0·110918
0·88	0·069006	—	0·068942	0·068963
0·9	0·057389	0·057629	—	0·057228
0·92	0·044675	—	0·045254	0·044295
0·94	0·029862	—	—	0·028807
x_{sep}	0·96	0·96	0·96	0·96

Horton's parabolic wall shear distribution

Horton[10] devised a parabolic distribution of f''_w to test the boundary layer equations in regions of small separation. His distribution of transformed wall shear is given by

$$S(\xi)=0{\cdot}4696(1-\xi)(1-0{\cdot}52649\xi), \quad \xi>0.$$

Separation occurs at $\xi=1$, with reattachment at $\xi=1{\cdot}9$. Because of its simplicity and the existence of a small separation bubble, this case was used as a test for all of the inverse options. The transformed wall shear method was used to generate input data for the other runs.

Figure 1 compares Horton's computational data with three inverse options (specifying f''_w, $\hat{\delta}^*$ and $C_{f_e}\sqrt{(Re)}$) from the present study. The agreement among all resullts is very good, although the displacement thickness run displays a slightly different trend from the other cases.

Two interesting discoveries were made while obtaining the displacement thickness runs. These were that accurate results could not be obtained without increasing the value of η_∞ obtained from the wall shear cases by 10–15%, and that two-point backward differences were necessary (rather than the usual three-point differences) over the ξ-interval where the flow separates. The requirement of increasing η_∞ indicates a finer sensitivity of the displacement thickness method to the location of the boundary layer edge. Oscillations in the normal velocity V occurred when the separated case was run using three-point backward differences for the entire domain. The cases where wall shear or skin friction coefficient distributions were specified did not exhibit these oscillations.

Figure 2 compares the computed $\delta^*\sqrt{(Re)}$ distribution from the inverse option specifying f''_w with the computational data of Horton. The agreement is exceptionally good, with essentially no deviation between the two curves.

Analytic displacement thickness distribution

Carter[13] developed an algebraic distribution of the untransformed displacement thickness $\delta^*\sqrt{(Re)}$ which matches the flat plate displacement thickness at the start and end of the

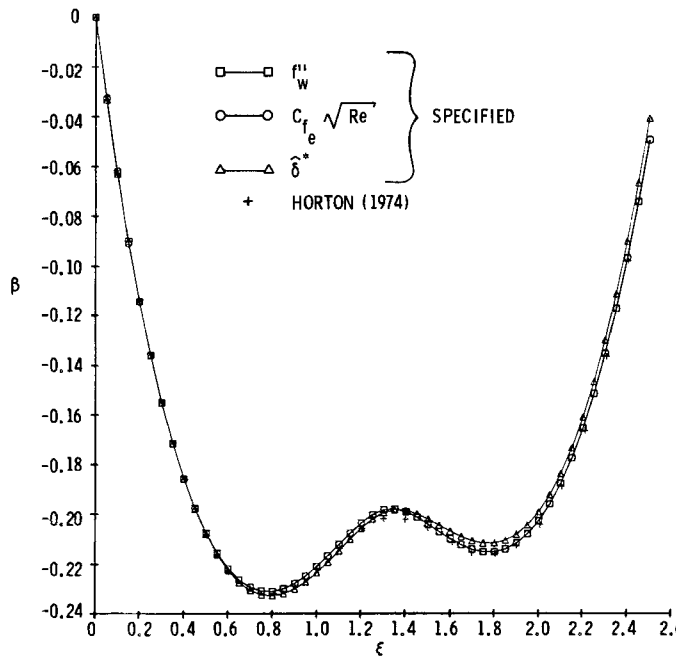

Figure 1. Comparison of pressure gradient parameter β from present inverse methods with Horton[10]

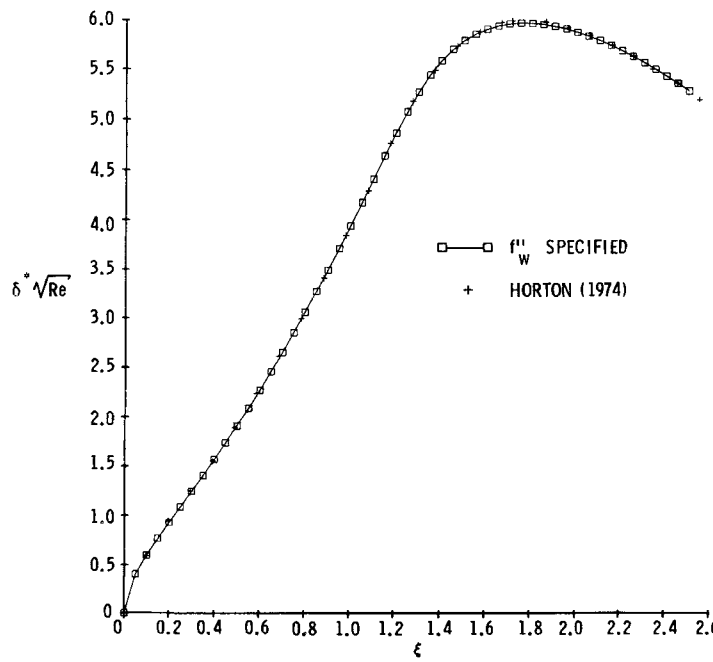

Figure 2. Comparison of scaled displacement thickness $\delta^*\sqrt{(Re)}$ with Horton[10]

distribution and reaches a maximum at a specified interior location. Carter uses this distribution to test a forward-marching scheme with FLARE as well as a global iteration scheme. Cebeci *et al.*[7] use the same distribution to test a marching solution with the iterative DUIT procedure for separation bubbles. The distribution is given in Reference 7. Two maximum values of displacement thickness are considered here, $\delta^*\sqrt{(Re)}=5{\cdot}6$ and $8{\cdot}6$, the same values cited in the above references.

The skin friction distribution resulting from the inverse option specifying $\delta^*\sqrt{(Re)}$ is compared with the computational results of Carter[13] and Cebeci *et al.*[7] in Figure 3. The agreement within the region of separation is particularly good, with the present method matching the global iteration results of Carter and the DUIT procedure of Cebeci *et al.* more closely than the forward-marching results presented by Carter. Figure 4 compares the edge velocity distribution for the same case with the global iteration results of Carter. Again the comparison is quite good, although the present solution overshoots the downstream flat plate value. The present prediction approaches the downstream flat plate value more closely as the streamwise step size is reduced.

For the more severe displacement thickness case, $\delta^*\sqrt{(Re)}=8{\cdot}6$, two-point backward differences had to be used in the separation bubble to obtain an accurate solution. A comparison of $C_{f_\infty}\sqrt{(Re)}$ distributions is made in Figure 5. Again the results are compared with those of Carter and Cebeci *et al.* The results compare well, although the overshoot behaviour is still evident. Decreasing the streamwise step size greatly increases the accuracy at the most negative value of f''_w. The edge velocity distribution from the same inverse runs is compared with Carter's global iteration results in Figure 6. Here, the present calculations fall slightly below the results of Carter. The overshoot behaviour is very apparent downstream of $x=1{\cdot}6$, shifting the minimum value of u_e upstream approximately 0·05 units.

The suspected cause of the overshoot behaviour is streamwise discretization error. To study this effect, the number of streamwise points was doubled. Figure 7, which compares the specified

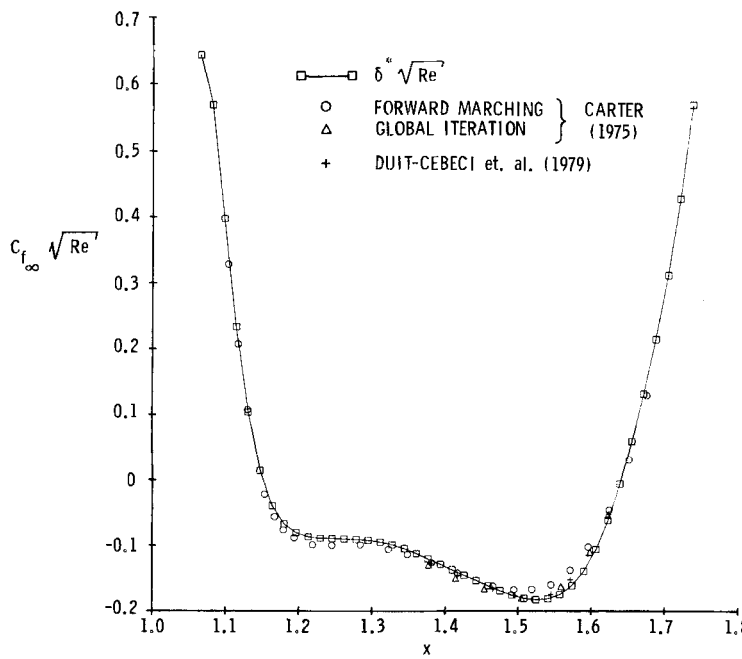

Figure 3. Comparison of $C_{f_\infty}\sqrt{(Re)}$ from present method with References7 and 13 for $\delta^*_{max}=8{\cdot}6$

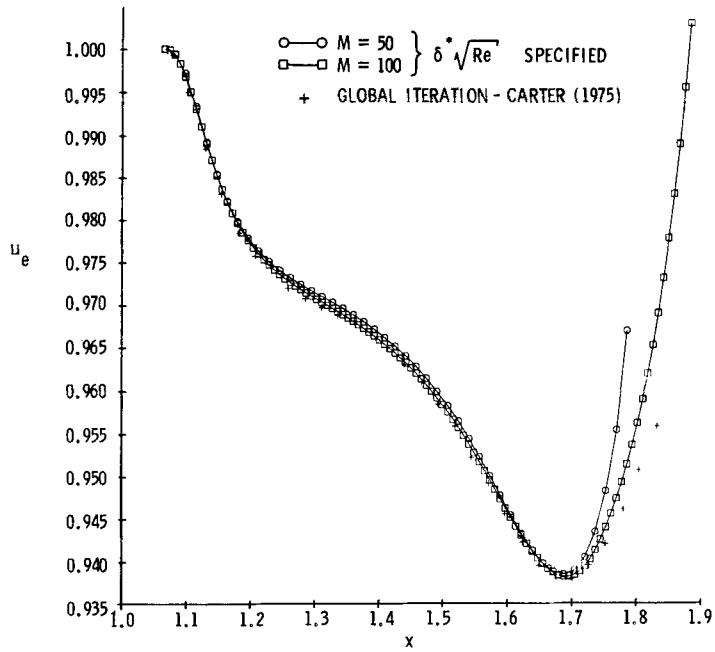

Figure 4. Edge velocity distribution for $\delta^*_{max}=5{\cdot}6$

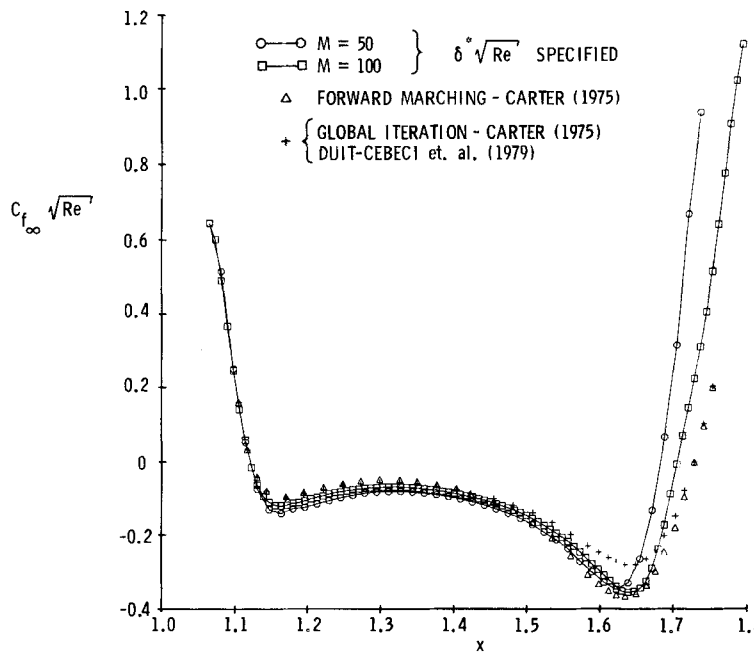

Figure 5. Comparison of $C_{f\infty}\sqrt{(Re)}$ with References 7 and 13 for $\delta^*_{max}=8{\cdot}6$

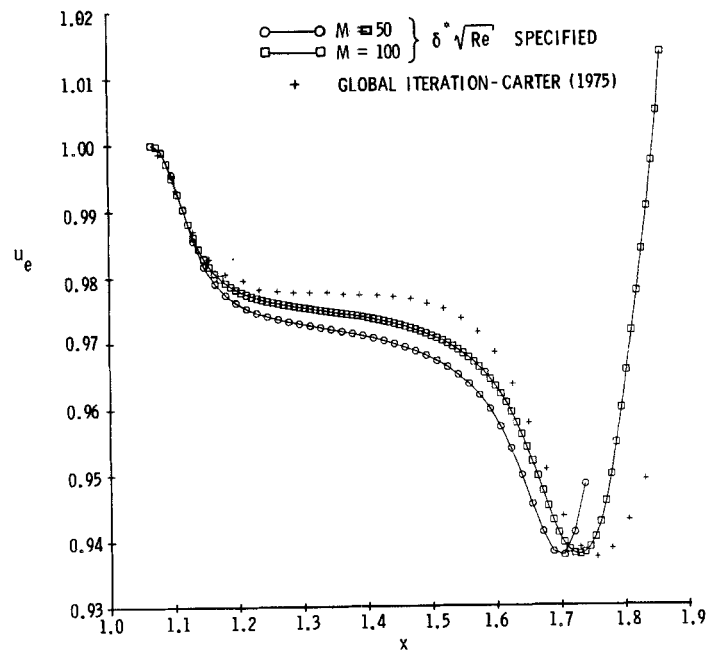

Figure 6. Edge velocity distribution for $\delta^*_{max}=8{\cdot}6$

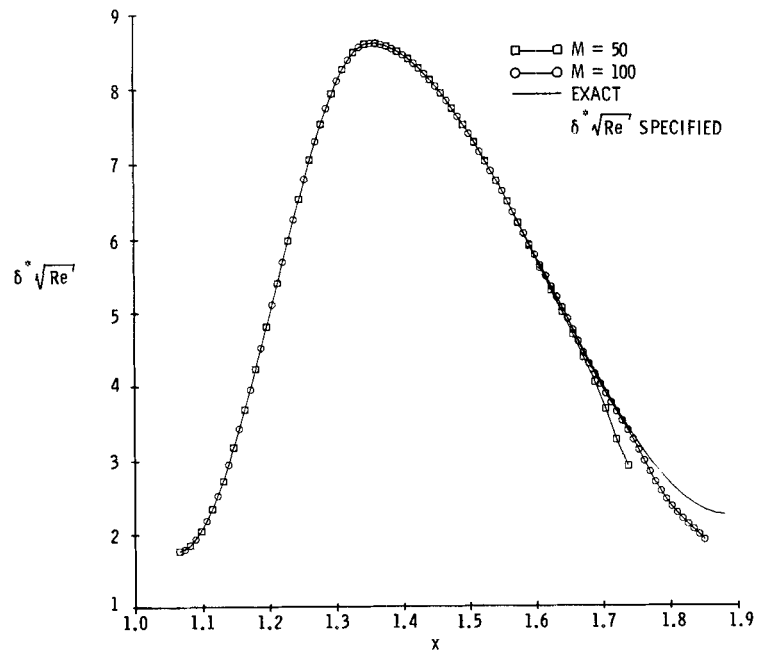

Figure 7. Scaled displacement thickness distribution for $\delta^*_{max}=8{\cdot}6$

displacement thickness with that calculated by the present shear method, shows the marked improvement obtained with the decrease in streamwise step size. The previous figures also demonstrate this effect.

DISCUSSION

Inverse wall shear methods

In the present investigation, three different inverse formulations for boundary layer flows have been studied. It should be noted that, aside from Horton,[10,11] this study is the only one known to the authors which formulates the inverse problem in full (streamwise and normal) Levy–Lees coordinates for separated flow. This study differs from those of Horton in the discretization and solution procedure followed once the equations are cast in psuedo-self-similar form.

The transformed wall shear method proved to be the most straightforward of the inverse formulations, requiring only an easily implemented boundary condition at the wall. This problem was covered in detail in Reference 18. The methods where the skin friction coefficients $C_{f_e}\sqrt{(Re)}$ and $C_{f_\infty}\sqrt{(Re)}$ are specified are of more practical importance. These methods required the development of specialized boundary conditions as discussed earlier in this paper. The use of these boundary conditions, which relate the quantities ξ and u_e to the pressure gradient parameter correction, is necessary to accelerate the convergence of the solution. The careful linearization of the boundary conditions was found to be very important to both the accuracy of the method and the rate of convergence. Without the linearized form of these conditions, convergence is achieved typically only after ten or more iterations. Proper linearization allows quadratic convergence to be maintained.

The wall shear formulations experience a problem with some separated flows. Flows which decelerate rapidly from positive to significant negative values of f''_w over a small streamwise distance cause the solution method to fail. This behaviour was observed when the shear methods were applied to the algebraic displacement thickness test problem of Carter.[13]

Upon examining the distributions of stream function f and velocity u across the boundary layer, an additional reflex in the stream function profile was found near the wall. This evidently leads to oscillations in the solution. A comparison of an incorrect profile of f near the wall with a correct profile for a similar separated region is shown in Figure 8. This failure seems to be inherent in the use of splines in combination with the boundary conditions applied at the wall for the shear formulations.

Based upon a comparison of results from the wall shear and displacement thickness methods, it is clear that an inherent difference in the formulation is responsible for the displacement thickness method's success in calculating regions of separation and the wall shear method's failure. This difference is in the form of the wall boundary conditions for the two methods. The wall boundary conditions for the wall shear methods only involve the variables f, u and G at $j=1$, with no dependence on $j=2$. Only the condition on β involves values at both $j=1$ and $j=2$, but this condition has no effect on the profiles of f, u and G.

The displacement thickness case does include a two-point spline boundary condition at the wall which links the values of f, u and G at points $j=1$ and $j=2$. This condition apparently forces the splines to behave in the correct manner near the wall when the flow separates, since the displacement thickness case was used successfully on all occasions. The lack of this two-point condition in the wall shear method allows the splines to 'wiggle' near the wall. This phenomenon seems to occur when the value of f''_w exceeds some undetermined limit near or following separation. This conclusion is based upon observed behaviour of the test cases. The methods also

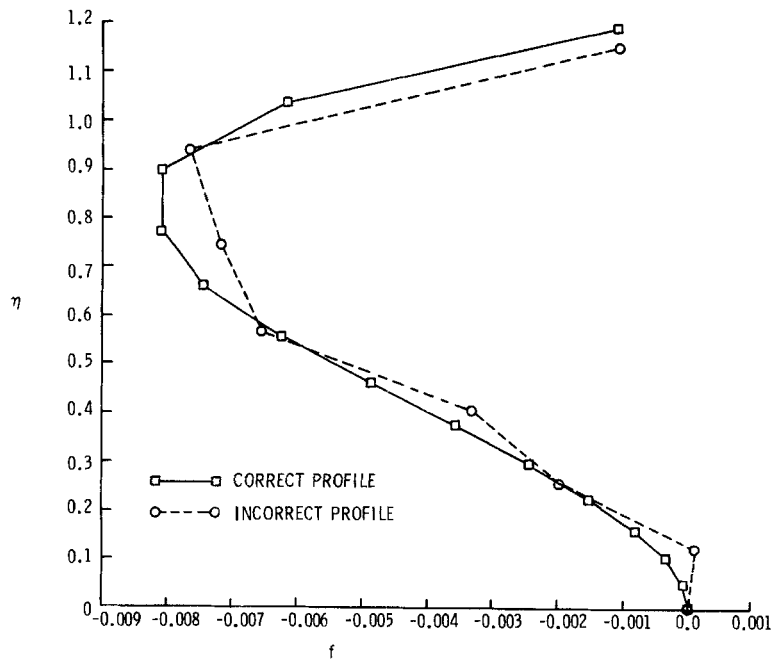

Figure 8. Comparison of incorrect and correct psuedo-self-similar stream function profiles near the wall

seem to fail when the backflow velocities become larger than 1% of the edge velocity. The inclusion of the two-point boundary condition for the displacement thickness method may also be the reason this method can handle separated zones with values of f''_w much larger (more negative) than the wall shear methods can tolerate. This explains why the wall shear methods perform well for mild cases, such as the Horton parabolic distribution, but fail for other problems, such as the separation bubble generated by Carter's analytical distribution of displacement thickness.

In the current formulation it is not possible to incorporate a two-point spline condition at the wall for the wall shear methods. Considering the conditions that exist at the wall, only the condition on β may be transferred to the outer edge, since the homogeneous conditions on f and u must remain at the wall, as must the inverse condition itself. Unfortunately, it was found that transferring the two-point condition on β to the far field produced oscillations there which occurred for attached and separated flow conditions and which significantly decreased marching distance. The conclusion is that for the present formulation the required two-point wall boundary condition, which would allow the wall shear methods to accurately handle larger regions of separation, cannot be implemented.

Despite the inability of the wall shear methods to handle larger regions of separation, the methods have proven to be very accurate for mild separated regions and for attached flows. It should also be pointed out that this limitation may be eliminated by switching from the use of fourth-order splines to a standard finite difference scheme.

Inverse displacement thickness method

The displacement thickness formulation proved to be the most successful of the inverse methods implemented in this study. This method provided reliable results for all cases, including those

which proved to be too severe for the wall shear methods. This is apparently due to the use of two-point spline conditions implemented at the wall, as discussed previously.

Several interesting observations were made during the use of the displacement thickness method. On several occasions a mild streamwise instability was noted when three-point backward differences were used. This instability was first noticeable through oscillations in the calculated normal component of velocity, which is dependent on f_ξ. For these cases it was necessary to switch to two-point backward differences over the region where separation was present. The use of two-point backward differences yields accurate solutions through separation without difficulty.

Another unexpected observed behaviour was overshoot of the solution following reattachment for the Carter analytic displacement thickness cases. The calculations should return to a flow with a near-zero pressure gradient, as for a flat plate. For the cases run, the calculations produce a flow which continues to accelerate following reattachment, overshooting the flat plate value of $\delta^*\sqrt{(Re)}$. The overshoot problem, while present for both displacement thickness distributions, is much more pronounced for the more severe distribution.

The suspected cause of this behaviour is streamwise discretization error, which is aggravated by the use of two-point backward differences. As a check, the streamwise step size was halved, as discussed in the Results section. These calculations show a marked improvement over the initial calculations, although the overshoot behaviour is still noticeable. The convergence behaviour of the present method was proven to be sensitive to accelerating flows, however, and this sensitivity may be the cause of the remaining discrepancies.

Direct method

The direct solution option of the present boundary layer formulation was tested using the Howarth flow as well as other standard test problems discussed in Reference 20. The method performed well for all test cases, with quadratic convergence consistently observed. Three to four iterations were typically needed at each streamwise station to converge the solution. Upon reaching negative values of f''_w, the solution diverged as expected.

The present direct method is interesting, since only two boundary conditions must be changed to switch the solution procedure from inverse to direct mode. To obtain a direct solution with the present formulation, β is specified and the inverse condition discarded. The direct method retains the 4×4 block structure of the inverse methods, with the mechul function equation on β simply becoming a 'dummy' equation. This suggests that the solution procedure could be easily switched from direct to inverse mode during calculations, although this was not attempted during the study.

Boundary conditions

Throughout the investigation, the methods developed have proven to be very sensitive to the boundary conditions. A prime example is the wall shear method for certain backflow conditions, as discussed previously. This behaviour was completely unexpected, since the boundary conditions applied at the wall are quite typical, except for the inverse condition. The use of the splines, however, is not typical.

Unexpected results related to the two-point spline relations were observed in other situations aside from the behaviour of the wall shear methods in separated flows. The oscillations produced by transferring the two-point condition on β from the wall to the far field are another instance of such behaviour. Although the boundary condition was expected to be satisfactory at the far field, the resulting oscillations caused the solution to diverge. Similar behaviour was observed for the boundary conditions in the direct method.

In all instances, the solution behaviour was found to be extremely sensitive to the particular implementation of the two-point spline relations. Often it was found that one condition adversely affected the solution while another provided accurate results, although both were expected to be adequate. The cause of this sensitivity is unclear from the results of the current investigation.

Pivoting

The present direct and inverse methods employ partial pivoting in the L–U decomposition to prevent the build-up of round-off errors. In an effort to determine whether an ideal ordering of the equations exists, the pivoting indices in the block matrix solver were observed during solution of a non-similar boundary layer flow. By checking these indices, it is possible to determine the pivoting elements of the L–U decomposition procedure. If the decomposition routine pivots consistently about the same elements, an ideal order of the equations is implied.

The check of the pivoting indices, however, shows no such consistency. Not only does the pivoting order change continually across the boundary layer, but it also changes as the solution proceeds downstream. This indicates that no predetermined order of the equations exists. Thus, regardless of the equation ordering, pivoting is an essential process for obtaining an accurate solution with the present formulation.

CONCLUDING REMARKS

A unified approach to calculating direct and inverse solutions for two-dimensional boundary layers has been presented. By a simple intercharge of boundary conditions, the method is capable of providing a direct solution, with a pressure distribution specified, or one of several inverse solution options, depending upon the specification of wall shear, skin friction coefficient or displacement thickness distributions. A modified form of the mechul function method is used to obtain the inverse solutions. Spline/finite difference discretization yields a fully implicit scheme which converges quadratically when proper linearization is applied.

Although the method usually performs quite well, it was discovered that the wall shear/skin friction coefficient options do not converge properly for separation regions with backflow velocities greater than 1% of the edge velocity. This behaviour is due to the nature of the splines, combined with the lack of the sufficiently strong two-point boundary condition at the wall for the shear options. Without proper control through the wall conditions, the splines allow oscillations in the solution profiles in regions of separation. The displacement thickness option, which does employ a strong wall boundary condition, is capable of treating regions of separation with larger backflow velocities (approximately 10% of the edge velocity).

The solution procedure is also sensitive to the use of the three-point backward differences, sometimes requiring the use of two-point backward differences for accurate results. This sensitivity appears mainly during the calculation of separated regions and is manifested by oscillations in the normal component of velocity. This sensitivity was also noted during the application of various forms of the two-point spline boundary conditions, with the most severe case occurring in the wall shear options. Here the sensitivity prohibits the use of the wall shear methods in separation regions which are not extremely mild. This sensitivity in the use of backward differences also appears in the overshoot noted with the analytic displacement thickness distributions. The behaviour of the method here is unsatisfactory and requires further investigation to eliminate any grid dependence. It should be noted, however, that grid-dependent behaviour was not observed elsewhere during the investigation.

These conclusions warrant further research into the use of the splines for regions of separation. It should be noted, however, that the spline formulation performed excellently in many instances,

yielding very accurate results with a minimum of grid points. The successful use of spline discretization for solutions involving reserved flow is tied to the use of strong two-point boundary conditions at the wall. Satisfactory results have been obtained only when such a condition is implemented. Unfortunately, this form of boundary condition is sometimes difficult to apply. To shed further light on the formulation and its problems, a complete stability analysis should be performed to determine the source of the encountered instabilities. While the present study indicates further work is required to resolve inadequacies in this method, the authors believe the investigation provides important information in obtaining boundary layer solutions with a unified algorithm.

ACKNOWLEDGEMENTS

This research was supported by the Naval Sea Systems Command and the Exploratory and Foundational Research Program at the Applied Research Laboratory of the Pennsylvania State University.

APPENDIX: NOMENCLATURE

A, B, C	4×4 block tridiagonal coefficients
C_f	skin friction coefficient $= \tau_w / \frac{1}{2} \rho_{ref} u_{ref}^2$
L^g	spline derivative approximation for $\partial^2 g / \partial \eta^2$
L	reference length
N	number of intervals in normal direction
R	column vector of known quantities
Re	reference Reynolds number $= \rho_\infty u_\infty L / \mu_\infty$
V	Reynolds scaled normal velocity component
Y	Reynolds scaled normal co-ordinate
Z	column vector of solution variable corrections
f	psuedo-self-similar stream function
h	normal step size in η
l^g	spline derivative approximation for $\partial g / \partial \eta$
p	pressure
u, v	untransformed streamwise and normal velocity components
x, y	untransformed streamwise and normal co-ordinates
δ^*	boundary layer displacement thickness
δ^*	transformed displacement thickness
δg	correction for variable g
τ_w	wall shear
ρ	fluid density
μ	dynamic viscosity
ν	kinematic viscosity
ψ	stream function
ξ, η	Levy–Lees streamwise and normal co-ordinates
β	streamwise pressure gradient parameter
θ	FLARE coefficient

Subscripts

e	edge value
i, j	spline/finite difference nodal points

w	wall value
∞	reference/freestream value
ξ, η	streamwise and normal partial derivatives

Superscripts

n	iteration level
*	dimensional quantity

REFERENCES

1. A. M. O. Smith, and D. W. Clutter, 'Solution of the incompressible laminar boundary-layer equations', *AIAA J.*, **1**, 2062–2071 (1963).
2. S. Goldstein, 'On laminar boundary-layer separation', *Quart. J. Mech. Appl. Math.*, **1**, 43–69 (1948).
3. S. N. Brown and K. Stewartson, 'Laminar separation', *Ann. Rev. Fluid Mech.*, **1**, 45–72 (1969).
4. D. Catherall and K. W. Mangler, 'Integration of the two-dimensional laminar boundary-layer equations past the point of vanishing skin friction', *J. Fluid Mech.*, **26**, Pt 1, 163–182 (1966).
5. T. A. Reyhner and I. Flugge-Lotz, 'The interaction of a shock wave with a laminar boundary layer', *Int. J. Non-Linear Mech.*, **3**, 173–199 (1968).
6. P. G. Williams, 'A reverse flow computation in the theory of self-induced separation', *Proc. Fouth Int. Conf. on Numerical Methods in Fluid Dynamics, Lecture Notes in Physics*, Springer–Verlag, 1975, pp. 445–451.
7. T. Cebeci, H. B. Keller and P. G. Williams, 'Separating boundary-layer flows: numerical determination of pressure gradient for a given wall shear', *J. Comput. Phys.*, **31**, 363–378 (1979).
8. H. B. Keller and T. Cebeci, 'An inverse problem in boundary-layer flows: numerical determination of pressure gradient for a given wall shear', *J. Comput. Phys.*, **10**, 151–161 (1972).
9. J. M. Klineberg and J. L. Steger, 'The numerical calculation of laminary boundary-layer separation', *NASA TN D-7732*, July 1974.
10. H. P. Horton, 'Separating laminar boundary layers with prescribed wall shear', *AIAA J.*, **12**, 1772–1774 (1974).
11. H. P. Horton, 'Comparisons between inverse boundary-layer calculations and detailed measurements in laminar separated flows', *Aeronaut. Quart.*, 169–187 (August 1981).
12. J. E. Carter, 'Solutions for laminar boundary layers with separation and reattachment', *AIAA Paper 74-583*, 1974.
13. J. E. Carter, 'Inverse solutions for laminar boundary-layer flow with separation and reattachment', *NASA TR R-447*, November 1975.
14. J. E. Carter, 'Inverse boundary-layer theory and comparison with experiment', *NASA TP-1208*, 1978.
15. T. Cebeci, 'An inverse boundary-layer method for compressible laminar and turbulent boundary layers', *J. Aircraft*, **13**, 709–717 (1976).
16. D. E. Edwards and J. E. Carter, 'A quasi-simultaneous finite difference approach for strongly interacting flow', in T. Cebeci (ed.), *Numerical and Physical Aspects of Aerodynamic Flows III*, Springer-Verlag, 1986.
17. S. G. Rubin and P. K. Khosla, 'Polynomial interpolation methods for viscous flow calculations', *J. Comput. Phys.* **24**, 217–244 (1977).
18. T. Cebeci and H. B. Keller, 'Laminar boundary layers with assigned wall shear', *Proc. Third Int. Conf. on Numerical Methods in Fluid Dynamics, Lecture Notes in Physics, Vol. 19*, Springer-Verlag, 1973, pp. 79–85.
19. K. C. Kaufman and G. H. Hoffman, 'Inverse laminar boundary-layer problems with assigned shear. The mechul function revisited', *Int. j. numer. methods fluids*, **5**, 1035–1045 (1985).
20. K.C. Kaufman, 'A unified direct–inverse procedure for two-dimensional boundary layers using spline/finite difference discretization', *Masters Thesis*, The Pennsylvania State University, 1986.
21. F. G. Blottner, 'Introduction to computational methods in boundary layers', *Sandia Report 79-083*, Sandia Laboratories, Albuquerque, NM, September 1979.
22. H. B. Keller, 'Numerical solution of two point boundary value problems', *Regional Conference Series in Applied Mathematics*, Society for Industrial and Applied Mathematics, 1976.
23. L. Rosenhead, *Laminar Boundary Layers*, Oxford University Press, Oxford, 1963.
24. P. Bradshaw, T. Cebeci and J. H. Whitelaw, *Engineering Calculation Methods for Turbulent Flow*, Academic Press, New York, 1981.
25. F. M. White, *Viscous Fluid Flow*, McGraw-Hill, New York, 1974.
26. L. Howarth, 'On the solution of the laminar boundary-layer equations', *Proc. Roy. Soc. London, Ser. A*, **164**, 547–579 (1938).
27. T. Cebeci and A. M. O. Smith, *Analysis of Turbulent Boundary Layers*, Academic Press, New York, 1974.